Carbohydrate Research 344 (2009) 901–907

Contents lists available at ScienceDirect

Carbohydrate Research

journal homepage: www.elsevier.com/locate/carres

Chitosan derivatives alter release profiles of model compounds from calcium phosphate implants

S. Green [a], M. Roldo [a], D. Douroumis [b], N. Bouropoulos [c,d], D. Lamprou [a], D. G. Fatouros [a,*]

[a] School of Pharmacy and Biomedical Sciences, University of Portsmouth, St. Michael's Building, White Swan Road, Portsmouth PO1 2DT, UK
[b] Department of Pharmaceutical Sciences, Greenwich University, Central Avenue, Chatham Maritime, Kent ME4 4TB, UK
[c] Department of Materials Science, University of Patras, Rio Patras 26504, Greece
[d] Foundation for Research and Technology, Hellas-Institute of Chemical Engineering and High Temperature Chemical Processes—FORTH/ICE-HT, PO Box 1414, GR-26504 Patras, Greece

ARTICLE INFO

Article history:
Received 10 November 2008
Received in revised form 8 February 2009
Accepted 17 February 2009
Available online 28 February 2009

Keywords:
Chitosan derivatives
Hydroxyapatite
Calcium phosphate implants
Calcein
FITC-dextran

ABSTRACT

The aim of the current study was to evaluate the impact of chitosan derivatives, namely *N*-octyl-chitosan and *N*-octyl-*O*-sulfate chitosan, incorporated in calcium phosphate implants to the release profiles of model drugs. The rate and extent of calcein (on M.W. 650 Da) ED, and FITC-dextran (M.W. 40 kDa) on in vitro release were monitored by fluorescence spectroscopy. Results show that calcein release is affected by the type of chitosan derivative used. A higher percentage of model drug was released when the hydrophilic polymer *N*-octyl-sulfated chitosan was present in the tablets compared with the tablets containing the hydrophobic polymer *N*-octyl-chitosan. The release profiles of calcein or FD from tablets containing *N*-octyl-*O*-sulfate revealed a complete release for FD after 120 h compared with calcein where 20% of the drug was released over the same time period. These results suggest that the difference in the release profiles observed from the implants is dependent on the molecular weight of the model drugs. These data indicate the potential of chitosan derivatives in controlling the release profile of active compounds from calcium phosphate implants.

1. Introduction

In the last 30 years, calcium phosphate (CaP) ceramics have become very popular implant materials for diverse clinical applications because of their similarities to human bones.[1] Within the family of CaP-ceramics the most popular contains hydroxyapatite (HAP, $Ca_{10}(PO_4)_6(OH)_2$) which is an inorganic material and the major constituent of natural bone. Due to its biocompatible and osteoconductive nature, HAP has been widely used as a drug delivery system.[2] Other components of CaP-ceramics are: β-tricalcium phosphate (β-TCP), biphasic calcium phosphate (BCP) and amorphous calcium phosphate (ACP). CaP-ceramics can be used for the delivery of a broad spectrum of compounds including anticancer drugs,[3,4] estrogens,[5,6] antibiotics,[7,8] insulin[9] and macromolecules such as bone morphogenic protein-2 (BMP-2),[10] transforming growth factor (TGF-β), basic fibroblast growth factor (b-FGF) and vascular endothelial growth factor (VEGF).[11,12]

A common approach to alter the release profile of active compounds from ceramics platforms is the addition of polymers such as polylactic acid-based polymers[13–16] and biopolymers such as collagen[17] and chitosan[18] which are physically or chemically mixed with a ceramic compound.

Chitosan is a natural polysaccharide derived by N-deacetylation of chitin. It is considered as a biocompatible and biodegradable polymer widely used in the food industry[19] and as a novel drug delivery platform for many routes of administration (e.g., nasal, oral, ophthalmic, buccal and parenteral).[20] However, chitosan has got a major drawback: its solubility is poor above pH 6 therefore, at physiological pH, chitosan will lose its capacity to enhance drug permeability and absorption, which can only be achieved in its protonated form. An approach to overcome this obstacle is to chemically modify the structure of chitosan by introducing hydrophilic groups or groups whose ionisation is pH independent.

In the present work, we have introduced the use of *N*-alkyl-*O*-sulfated chitosan. Sulfated chitosan possesses a wide range of biological activities such as anticoagulant, antiviral and antisclerotic activity, this is due to its structural similarity to the natural anticoagulant heparin;[21] the use of a sulfated derivative of chitosan could therefore improve the biocompatibility of the implant. Furthermore, modifying the sulfated chitosan by adding long alkyl chains to the amino group at C-2 induces the creation of an amphiphilic molecule that forms micelles in water and therefore offers the potential to increase the solubility of poorly soluble drugs. *N*-octyl-*O*-sulfate can therefore be used as a potential drug carrier.[22]

The aim of this study was to investigate the impact of chitosan, *N*-octyl-chitosan and *N*-octyl-*O*-sulfate chitosan on the release profile of two model drugs from biodegradable implants, composed of

* Corresponding author. Tel.: +44 23 9284 3929; fax: +44 23 9284 3565.
E-mail address: dimitris.fatouros@port.ac.uk (D.G. Fatouros).

0008-6215/$ - see front matter © 2009 Elsevier Ltd. All rights reserved.
doi:10.1016/j.carres.2009.02.022

tricalcium phosphate/hydroxyapatite blends. Calcein (M.W. 650 Da) was chosen as a model for low molecular drugs such as antibiotics that are often co-administered with other drugs when implants are put in place. FITC-dextran (M.W. 40 kDa) was chosen as a model for high molecular weight drugs such as proteins and peptides. In some cases, methylcellulose was also added to the implants.

2. Experimental

2.1. Materials

Low-viscous chitosan, cholsulfonic acid, sodium hydroxide (NaOH) and tricalcium phosphate (β-$Ca_3(PO_4)_2$) were purchased from Fluka Biochemika UK. Methanol (MeOH), dimethylfomamide (DMF), sodium chloride (NaCl) and sodium azide (NaN_3) were provided by Fisher Scientific, UK. Octaldehyde was from Aldrich UK, whilst sodium borohydrate ($NaBH_4$) was purchased from Acros Organics UK. Calcein, fluorescein isothiocyanate dextran (FITC dextran M.W. 40 kDa, FD) and methylcellulose (MC) were obtained from Sigma Aldrich. Potassium chloride (KCl), potassium di-hydrogen orthophosphate (KH_2PO_4), di-sodium hydrogen orthophosphate anhydrous (Na_2HPO_4) and calcium chloride ($CaCl_2$) were all purchased from BDH Chemicals Ltd, UK.

2.2. Preparation of hydroxyapatite

The hydroxyapatite (HAP) used in this study was prepared using the process, based on the precipitation of HAP from precursor compounds in aqueous solutions with slight modifications.[23] Briefly, calcium chloride solution of 0.5 M was added slowly to a 250 mL of 0.3 M disodium hydrogen phosphate under magnetic stirring at 80 °C. The pH of the solution was maintained between 9 and 10 by the addition of sodium hydroxide solution. The precipitate was washed with ultra pure water for several times and dried at 200 °C, under vacuum.

2.3. Characterisation of hydroxyapatite phosphate with XRD and FT-IR

Characterisation of the solid was made by FTIR spectroscopy (Excalibur, Digilab) and X-ray powder diffraction (XRD Siemens/Bruker D5000, Bruker GmbH, Germany, λ = 1.54 Å).

2.4. Synthesis of chitosan derivatives

2.4.1. *N*-Octyl chitosan

N-Octyl-*O*-chitosan was synthesised as previously described[22] with slight modification (Fig. 1). Briefly, chitosan (1.0 g) was suspended in methanol (50 mL) and octaldehyde (1.02 g) was added to the suspension while stirring; the suspension obtained was stirred at room temperature for 24 h. An aqueous solution of $NaBH_4$ (0.5 g in 5 mL) was slowly added to the reaction mixture and the resulting mixture was stirred at room temperature for further 24 h. The reaction was stopped by neutralisation with 2 M HCl. The product was filtered and repeatedly washed with methanol and water and finally dried under vacuum at 60 °C to constant weight (1.32 ± 0.02 g, n = 4).

2.4.2. *N*-Octyl-*O*-sulfate chitosan

N-Octyl-chitosan (1.0 g) was suspended in DMF (40 mL). Chlorosulfonic acid (20 mL) was added dropwise to 40 mL of DMF and the mixture was stirred for 1h at 0 °C. Then the *N*-octyl-chitosan suspension was added to the above solution. The mixture was reacted at 40 °C for 24 h. The reaction was stopped by neutralisation with 20%w/v NaOH, the obtained precipitate was filtered off and the filtrate was dialysed against distilled water for 3 days and then freeze dried (598.0 ± 16.1 mg, n = 3).

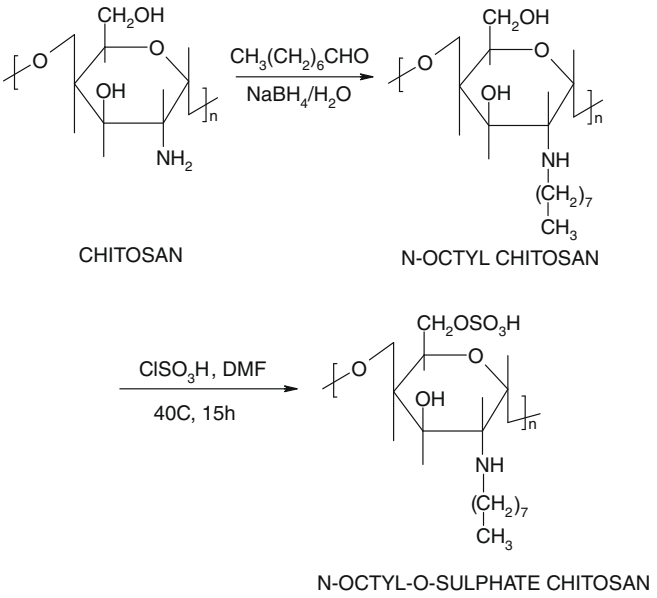

Figure 1. Synthesis of *N*-octyl-*O*-sulfate chitosan.

2.4.3. Characterisation of chitosan derivatives

Chitosan derivatives were characterised by the following methods. ^{1}H NMR spectra were obtained on a JEOL 400 MHz spectrometer operating at 400 MHz. The samples were dissolved in D_2O and TMS was used as a standard. ATR spectra were recorded on a Tensor 27 FTIR spectrophotometer. X-ray diffraction studies were conducted on a Philips X-ray diffractometer. Elemental analysis was carried out with a Carlo-Erba CHNS Elemental Analyzer EA1108.

2.5. Preparation of tablets

The ceramics tablets were prepared by mixing in a glass dish the appropriate amount of HAP and TCP keeping it constant in ratio (HAP:TCP, 25:75 w/w) with either chitosan or chitosan derivatives or methylcellulose where appropriate. In all cases the amount of polymer added was 0.19 g and the active compound was 0.03 g for calcein and 0.002 g for FITC-dextran 40 kDa. After the addition of 0.77 mL of deionised water a slurry paste was prepared and placed in the vacuum oven at 60 °C for 2 h and then left overnight at 40 °C.

Tablets with a weight of 200 mg each were prepared by compression, using a Specac hydraulic press by applying 3.5 tons for 5 min at room temperature.

2.6. Morphological observations of the implants

Scanning electron microscopy (JSM-6060LV, JEOL Ltd, Japan) was used to create 3-dimensional images of tablets surfaces.

2.7. In vitro release studies

The in vitro release profiles of calcein and FITC-dextran were obtained by using a dissolution apparatus with a method based on the official BP method, with modifications.[24] A dissolution apparatus was set up with six vessels containing 500 mL of PBS, pH 7.4 each; all vessels were covered with parafilm to avoid evaporation of the buffer. At scheduled time intervals, a 5 mL aliquot of

Table 1
Applied release models

Model	Equation
Baker–Lonsdale	$\frac{2}{3}\left[1-(1-\frac{F}{100})^{\frac{2}{3}}\right]-(\frac{F}{100})=kt$
First order	$F=100(1-e^{-k_1 t})$
Higuchi	$F=k_H\sqrt{t}$
Hixson–Cromwell	$F=100[1-(1-k_{HC}t)^3$
Peppas	$F=k_p t^n$

F, amount of drug released in time t, k_{LB}, k_1, k_H, k_{HC}, k_P release rate constants, n release exponent.

the aqueous solution was withdrawn and replaced immediately with fresh buffer. Calcein and FITC dextran release was assayed by fluorescence spectroscopy. The samples were excited at 495 nm and their emission was measured at 515 nm for calcein and at 520 nm for FITC-dextran.

2.8. Kinetic studies and statistical analysis

Calcein and FITC-dextran release profiles were analysed by various mathematical models using SIGMAPLOT 10.0 software (Systat Software Inc., Germany). All the models tested are depicted in Table 1. Furthermore, the GRAPHPAD INSTAT® (GraphPad Software Inc., San Diego, US) was applied to assist the analysis of the dissolution profiles. This was carried out applying Mann-Whitney, non-parametric test and the two-tailed P value. Additionally, the Friedman non-parametric test followed by the Dunn post hoc

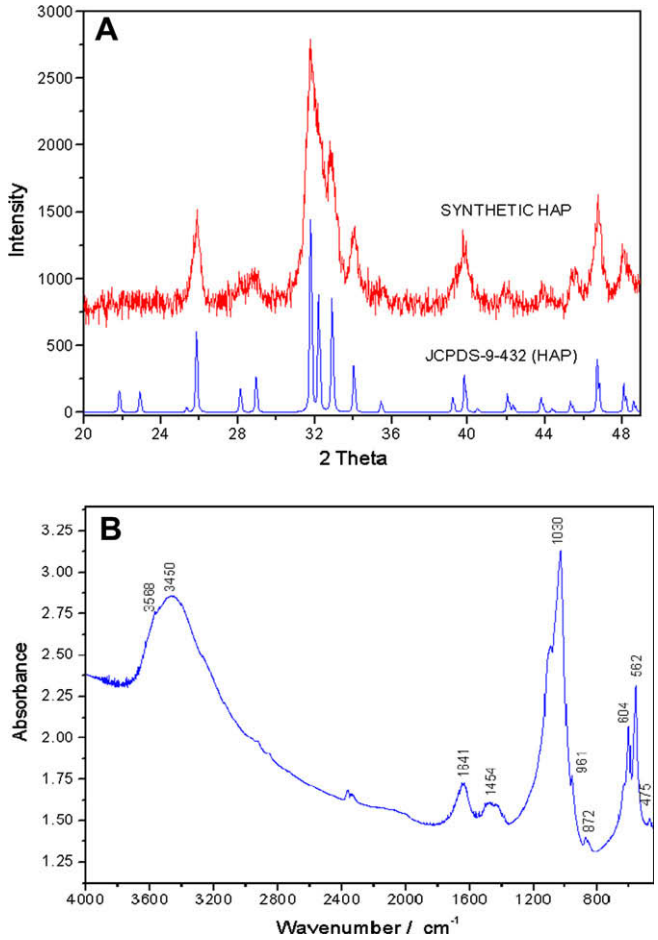

Figure 2. (A) XRD patterns of synthetic apatite and JCPDS File No. 09-432 B. FTIR spectrum of synthetic hydroxyapatite.

Table 2
Elemental analysis data and calculated degree of modification for chitosan and its derivatives

	Chitosan	*N*-Octyl-chitosan	*N*-Octyl-*O*-sulfate chitosan
% Nitrogen	7.19 (8.47 by NMR)[a]	5.06	4.12
% Carbon	40.30 (45.05 by NMR)[a]	54.13	35.41
% Hydrogen	6.45 (6.78 by NMR)[a]	9.17	5.48
% Sulfur	—	—	8.40
% Acetyl monomer	19.86	19.86	19.86
% Deacetylated monomer	80.14	15.79	15.79
% *N*-Octyl monomer	—	64.35	64.35
Average number of sulfate groups per monomer	—	—	0.78

[a] See Ref. 38.

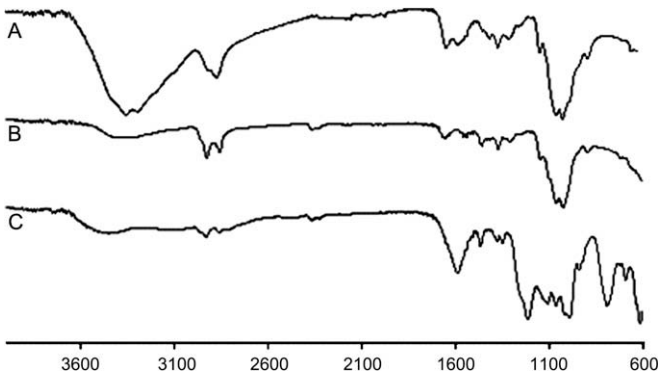

Figure 3. ATR spectra of (A) low viscous chitosan; (B) *N*-octyl chitosan; (C) *N*-octyl-*O*-sulfate chitosan.

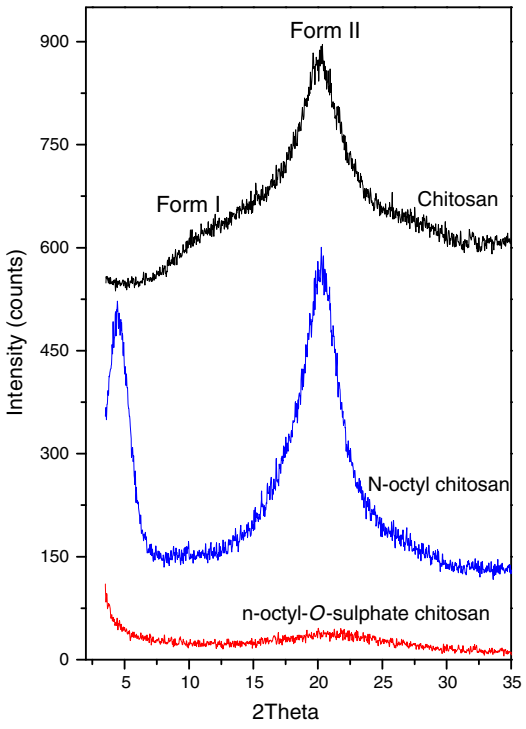

Figure 4. XRD patterns of chitosan and its derivatives.

multiple comparison test was also used to investigate any significant differences between the formulations.

3. Results and discussion

3.1. Characterisation of the hydroxyapatite

The X-ray diffractogram and the FT-IR spectrum of synthetic hydroxyapatite are depicted in Figure 2. The XRD did not show the presence of the crystalline phases. The measured XRD pattern for the synthesised HAP showed reflections which are in agreement with those of the JCPDS File No. 09-432 (standard) (Fig. 2 A). The broadening of the peaks gave evidence that crystals have nanometer dimensions.

The FT-IR spectrum showed characteristic vibration peaks corresponding to PO_4^{3-} (562, 604, 1030 cm^{-1}) and OH^- stretching mode at 3568 cm^{-1} (Fig. 2B). The broad peak at 3450 is assigned to OH^- due to absorbed water. The presence of the peaks at 1454 cm^{-1} and 872 cm^{-1} is attributed to CO_3^{2-} groups. The presence of traces of carbonate ions is due to contamination since the preparation process was carried out under ambient atmosphere.

3.2. Characterisation of chitosan derivatives

N-Octyl-chitosan was successfully obtained in the form of a white water-insoluble powder, the reaction yield was highly reproducible (64.5 ± 0.9% w/w, $n = 4$). The attachment of the octyl chains to the primary amino group of chitosan was confirmed by FTIR analysis. The characteristic peak attributed to the bending vibration of $-NH_2$ (1587 cm^{-1}) disappeared from the FTIR spectra of the acylated derivative, whilst new peaks attributed to the octyl chain were evident (1649, 1537, 1465 and 1373 cm^{-1}). The degree of modification of the free amino groups was calculated from the elemental analysis data (Table 2) that confirmed successful acylation of 80.3% of the free amino groups. Furthermore, modification is also visible on the ^1H NMR spectrum (not shown) that shows acylation with appearance of new peaks at 0.8–1.0 ppm (–NH–CH_2–$(CH_2)_6$–CH_3), 1.2–2.0 ppm (–NH–CH_2–$(CH_2)_6$–CH_3) and 3.4–3.5 ppm (–NH–CH_2–$(CH_2)_6$–CH_3).

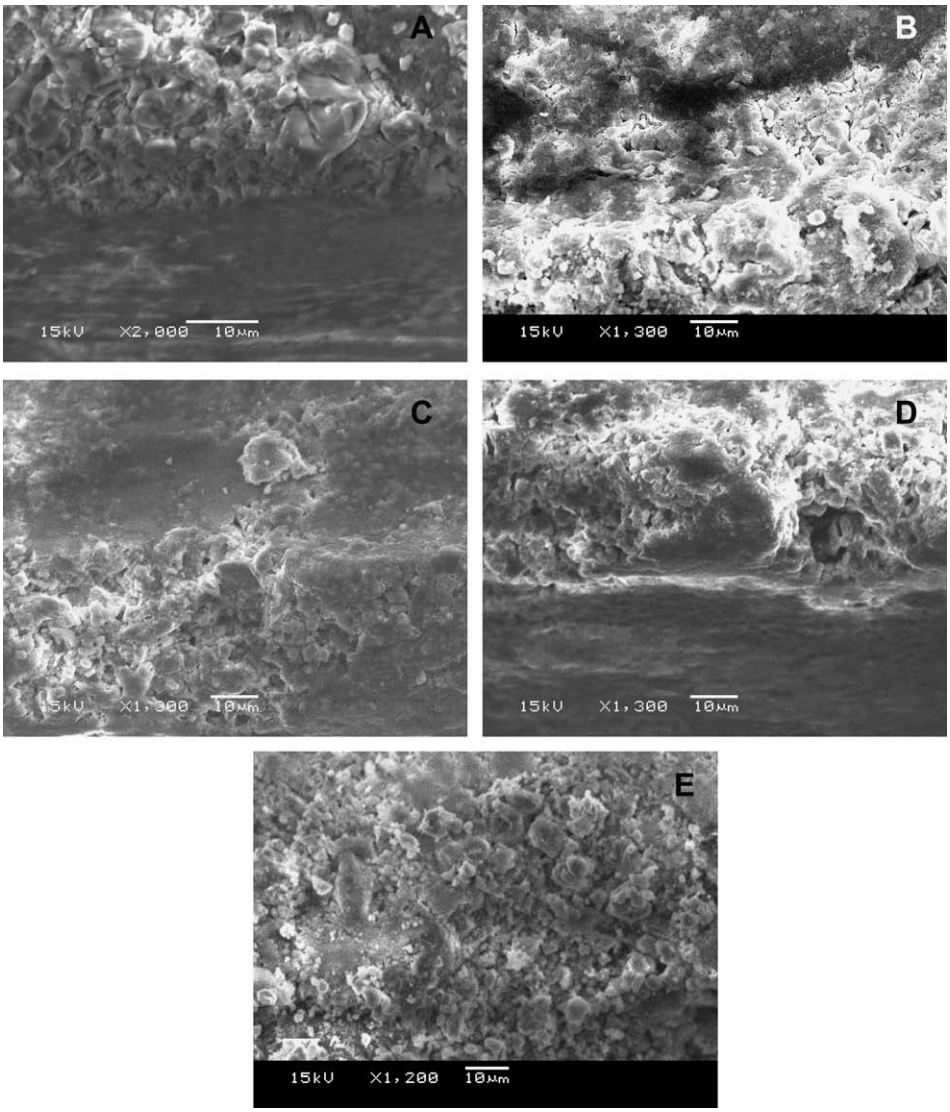

Figure 5. SEM images of different implants; (A) TCP:HAP implant containing chitosan and methylcellulose; (B) TCP:HAP implant containing *N*-octyl-chitosan; (C) TCP:HAP implant containing *N*-octyl-sulfate chitosan; (D) TCP:HAP implant containing *N*-octyl-sulfate chitosan and methylcellulose implant; (E) TCP:HAP and chitosan implant, bar represents 10 μm.

Sulfation of *N*-octyl-chitosan afforded a water soluble, off-white material. FTIR analysis revealed that *O*-sulfation occurred mainly at the hydroxylic group in position C6 as the peak attributed to the combination of O–H bending and C–O stretching of the primary alcohol (1166 cm^{-1}) disappeared and new peaks assigned to O═S═O appeared at 1268, 1200, 1095, 779 cm^{-1} (Fig. 3). Sulfation afforded an average of 0.78 sulfate groups per monomer (Table 2), this has been calculated assuming that the sulfation reaction does not affect the number of octyl- or acetyl-groups present on the polymer.

XRD spectra of chitosan and its derivatives are depicted in Figure 4. Pure chitosan exhibits a sharp peak at $2\theta = 20°$ and a weak peak at $2\theta = 11°$ which correspond to type II and type I crystal structure, respectively.[25] In the pattern of *N*-octyl chitosan a new sharp peak was observed at 4.4° while the peak at 11° disappeared. The result is in a good agreement with previous study which shows shifting of diffraction peak at 11° towards lower angles in the case of *N*-octyl chitosan.[26] Another systematic study of Muzzarelli et al. for *N*-alkyl-chitosan derivatives also showed that shifting of the first peak was analogous to the length of the alkyl group.[27] Finally, in the case of *N*-octyl-*O*-sulfate chitosan the diffraction peaks are weak indicating that crystallinity is almost lost. This suggest that introduction of sulfate groups in the alkyl chain lowers the ability to form intermolecular hydrogen bonds causing the polymer to become amorphous.

3.3. Morphological characterisation of the implants

Scanning electron images of different tablets were obtained after their manufacturing. Figure 5 illustrates the different compositions. Calcium phosphate tablets containing chitosan and MC are depicted in Figure 5A. Both rough, indicative of a semi-crystalline poorly water soluble molecule like chitosan, and smooth areas could be visualised. Large crystals characteristic of tricalcium phosphate were also frequently present. When *N*-octyl-chitosan was incorporated into the tablets, rough surfaces and crystalline structures were the dominant features (Fig. 5B). This is in accordance with the enhanced crystal organisation observed by XRD for this polymer compared to chitosan (Fig. 4). Smooth and rough areas could be visualised when *N*-octyl-*O*-sulfate chitosan with or without MC were present in the implants (Fig. 5C and D, respectively). Finally, implants containing only chitosan exhibit rough surfaces with crystalline structures (Fig. 5E).

3.4. Drug release studies

The release profiles of calcein from tablets containing chitosan with MC, *N*-octyl-chitosan and *N*-octyl-chitosan with MC are illustrated in Figure 6A. The presence of chitosan and MC significantly limited the diffusion of calcein from the tablets resulting in a release of only 9.73 ± 1.27% of the loaded drug, even after 120 h. This could be due to the ionic interaction between the negatively charged calcein molecule and the partially positive charged amino group of chitosan; furthermore, the presence of MC acts as a diffusion barrier slowing down the diffusion of the water inside the implant and delaying the release of the drug. On the other hand, the presence of the *N*-octyl-chitosan with and without MC in the tablets resulted in a significantly higher amount of calcein released compared with the formulation containing only chitosan ($p = 0.025$). More specifically, when *N*-octyl-chitosan was present in the tablet a fast release of calcein was observed during the first 2 h, followed by a decrease in the release rate that was then maintained constant up to 200 h, reaching a final value of 46.65 ± 9.39%. In the presence of MC no release occurred during the first 2 h, confirming the role of MC as a diffusion barrier. However, after 120 h the total amount of drug released reached 42.8 ± 4.88%. The

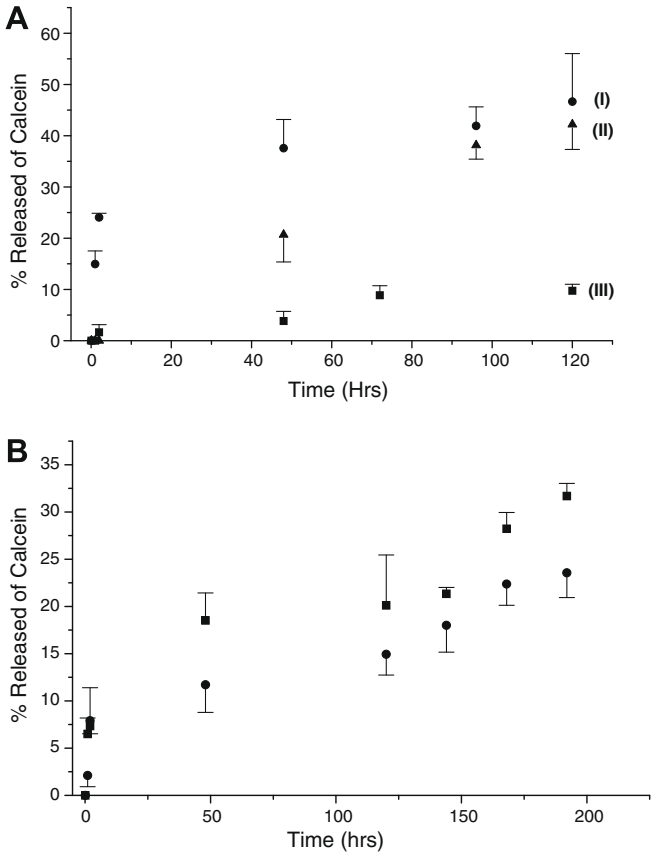

Figure 6. (A) Release profiles of calcein into PBS pH 7.4 from tablets TCP:HAP (75:25 w/w) containing (i) chitosan with MC (■), (ii) *N*-octyl-chitosan (●) and (iii) *N*-octyl-chitosan with methylcellulose (▲); (B) Release profiles of calcein into PBS pH 7.4 from tablets HAP:TCP (75:25 w/w) containing (i) *N*-octyl-sulfate chitosan (■) and (ii) *N*-octyl-chitosan with methylcellulose (●), each experiment was performed in triplicate and results are reported as mean ± standard deviation.

substitution of the hydrophilic polymer chitosan with its more hydrophobic derivative *N*-octyl-chitosan induced a decrease in the affinity of the drug for the implant that can be seen as the reason for the higher release observed. Furthermore, the semicrystalline nature of the polymer is likely to induce formation of hydrophilic and hydrophobic areas within the tablet; the hydrophobic areas are probably responsible for the quick release observed during the first hours, whilst the following constant rate is due to the controlled hydration of the hydrophilic areas. The addition of MC did not affect the total amount of drug released during the observed time ($p = 0.5068$); however, MC seemed to provide a more controlled drug release profile with an initial lag time of around 2 h. These results suggest that MC is a good excipient to add to the formulation in order to obtain a good control of release rate in a prolonged release system.

The effect of the *N*-octyl-*O*-sulfate chitosan and MC to the release of calcein is depicted in Figure 6B. The graph shows a quick release of calcein from both formulations during the first 2 h that could be due to the repulsion between the two negatively charged molecules; this was followed by a decreased release rate up to 200 h. Overall, the amount of drug released, when *N*-octyl-*O*-sulfate chitosan was added, achieved 31.69 ± 1.33% which is significantly higher ($p = 0.0087$) compared with the amount of drug released when MC was also present in the tablet (23.56 ± 2.62%); also in this case MC showed to have a role in controlling and slowing the drug release rate.

The lower percentage of drug released when the *N*-octyl-*O*-sulfate chitosan was present in the tablets compared with the tablets containing the *N*-octyl-chitosan could be attributed to the fact that

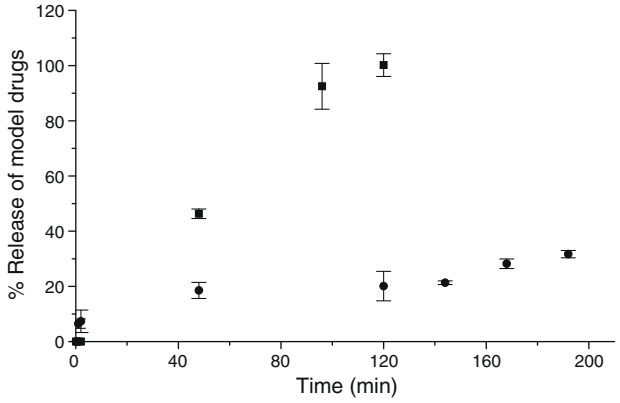

Figure 7. Release profiles from tablets TCP:HAP (75:25 w/w) and *N*-octyl-sulfate chitosan containing (i) FITC dextran (■), (ii) calcein (●), into PBS pH 7.4, each experiment was performed in triplicate and results are reported as mean ± standard deviation.

the sulfated derivative is more hydrophilic and presents a higher affinity for the model drug; furthermore, the amorphous structure of this polymer will form smaller pores within the implants compared to the two semicrystalline polymers making diffusion of calcein through the matrix slower. In general, it was observed that increasing the hydrophilicity of the polymers in the formulations, for example, addition of MC or use of the sulfated derivative instead of the alkylated one, resulted in a slower release rate of calcein affording implants with great potential in applications that require constant drug delivery over a prolonged period of time.

In order to study the effect of the implant formulation on the delivery of large molecules, the release profile of FD from calcium phosphate implants containing chitosan and *N*-octyl-*O*-sulfate chitosan was investigated. The release rate of this large molecule was expected to be slower and to reach lower levels compared to calcein. However, implants containing chitosan showed a fast diffusion of the drug with 100% release obtained after 2 h (data not shown).

This could be explained by the fact that during preparation of the implants all components are mixed with water to form a paste from which the water is successively evaporated. FD, being a hydrophilic polymer, would coordinate several molecules of water around its backbone which upon drying leave big pores that might favour the release of the model drug. When the hydrophilicity of the system was increased by the use of *N*-octyl-*O*-sulfated chitosan a more controlled release was obtained; no release occurred during the first 2 h and complete release of FD required 120 h. The slower release of FD when the sulfated chitosan derivative is present in the implant compared with the one containing chitosan could be due to the difference in crystallinity of the two compounds. The amorphous structure of *N*-octyl-*O*-sulfate chitosan could lead to better compaction of the tablet and slower release of the active compound. This is in line with the electron microscopy images obtained previously where both smooth and rough areas could be visualised when *N*-octyl-*O*-sulfate chitosan (Fig. 5C) was present in the implant compared with the extended rough surface of the implant containing only chitosan.

The release pattern of calcein or FD from tablets containing *N*-octyl-*O*-sulfate is depicted in Figure 7. Complete release was achieved for FD after 120 h compared with the calcein where only 20% of the drug was released in the same time period. These results suggest that the difference in the release profiles observed from the implants is also dependent on the molecular weight of the model drugs.

The release profiles in Figure 6A and B were statistically compared to determine whether a significant difference exists. This was carried out through the Mann-Whitney non-parametric test followed by a two-tailed P post test. In both cases the P values were 0.5285 (Fig. 6A) and 0.1464 (Fig. 6B), indicating non significant difference ($p > 0.05$). For Figure 6A, the Friedman non-parametric test was applied followed by Dunn's post test. The P (0.0062) value showed significant difference only for (I) versus (II) dissolution profiles while for pairs (I) versus (III) and (II) versus (III) it was found to be $p > 0.05$.

3.5. Drug release kinetics

The release profiles were fitted to several kinetics models. The parameters calculated by these models and the determination coefficients (R^2) obtained are summarised in Table 3. The Peppas[28] and Hixson–Crowell model[29] were able to fit most of the formulations where relative good coefficients were obtained (Table 3). Generally, in spherical matrices, if $n \leqslant 0.43$, a Fickian diffusion (case-I) is applicable, when $0.43 < n < 0.85$, a non-Fickian transport takes place and if $n \geqslant 0.85$, a case-II transport (zero order) drug release mechanism dominates.[28–31] All the other models such as first order,[32–34] Baker–Lonsdale[35] were able to fit the release profiles of both calcein and FD in one occasion each. These findings indicate that most of the release patterns are controlled by drug diffusion (Higuchi or Peppas) and surface of the tablet (Hixson–Crowell). The selection of the adequate model was based on comparisons of the following features for each model: higher determination

Table 3
Release rate constants and determination coefficients of the produced formulation

Dissolution models		Cal/C	Cal/NCO	Cal/NCO/MC	Cal/NCSO	Cal/NCSO/MC	FD/C	FD/NCSO
Baker–Lonsdale	K_{BL} (min^{-1})	0.0009 ± 0.0002	0.0005 ± 0.0001	0.0003 ± 0.0000	0.0001 ± 0.0000	0.0000 ± 0.0000	0.1298 ± 0.0609	0.0021 ± 0.0006
	R^2	0.9638	0.8591	0.9769	0.9510	0.9574	0.9347	0.9570
First order	k_1 (h^{-1})	0.0008 ± 0.0001	0.0062 ± 0.0016	0.0048 ± 0.0001	0.0020 ± 0.0002	0.0015 ± 0.0001	1.3402 ± 0.2528	0.0189 ± 0.0032
	R^2	0.8824	0.6577	0.9987	0.8830	0.9135	0.9877	0.9827
Higuchi	k_H (% min^{-1})	0.5649 ± 0.3678	4.6085 ± 0.5951	3.6668 ± 0.2333	2.113 ± 0.1345	1.615 ± 0.0979	67.219 ± 8.7919	8.7041 ± 0.6148
	R^2	0.9448	0.8349	0.9813	0.9492	0.9572	0.9498	0.9772
Hixson–Cromwell	k_{HC} ($min^{-1/3}$)	0.0003 ± 0.0001	0.0018 ± 0.0004	0.0015 ± 0.0000	0.0006 ± 0.0001	0.0005 ± 0.0000	0.3576 ± 0.0575	0.0050 ± 0.0005
	R^2	0.8822	0.6360	0.9979	0.8795	0.9116	0.9875	0.9913
Peppas	k_P (min^{-n})	0.680 ± 0.1567	14.775 ± 3.1316	0.8934 ± 0.3189	4.9091 ± 1.6651	2.9944 ± 1.3154	64.134 ± 15.0648	1.7456 ± 0.7952
	n	0.449 ± 0.0756	0.238 ± 0.0496	0.812 ± 0.0769	0.3291 ± 0.0688	0.3750 ± 0.0882	0.6185 ± 0.3630	0.8547 ± 0.0991
	R^2	0.947	0.964	0.9978	0.9669	0.9367	0.9577	0.9968

Cal: Calcein.
C: Chitosan.
NCO: *N*-octyl-chitosan.
MC: Methylcellulose.
NCSO: *N*-octyl-sulfate chitosan.
FD: FITC-dextran (4 kDa).

coefficient; smaller standard error of model parameters and smaller residual mean square.[36]

Dissolution profiles described by the Hixson–Crowell cube law are applied when the geometric shape of the dissolving particles diminishes proportionally over time, and when the dissolving particles are isometric. In this case, the drug release rate is proportional to the surface area of dosage form such as the erosion-dependent release systems. It is possible that the rough surface observed in the presence of *N*-octyl-*O*-sulfate chitosan inducing tablet erosion with the elapse of time and the tablet fragments were discharged in the dissolution medium.

The smooth surfaces observed in the presence of *N*-octyl-*O*-sulfate chitosan or methylcellulose are well fitted to the Peppas, Higuchi, Baker–Lonsdale and first-order models indicating diffusion dependence in every occasion caused by the polymer nature and close packing of the excipients.[37]

4. Conclusions

Our results demonstrate that the presence of different chitosan derivatives can alter the release profiles of model drugs depending on the intended use of these formulations. By tailoring the properties of the polymers (hydrophilic/hydrophobic) the desired drug release rate can be obtained. These preliminary results lay the framework for future work by employing biodegradable chitosan derivatives for bone implants.

References

1. Habraken, W. J. E. M.; Wolke, J. G. C.; Jansen, J. A. *Adv. Drug Delivery Rev.* **2007**, *4–5*, 234–248.
2. Lassare, A.; Bajpai, A. K. *Crit. Rev. Ther. Drug Carr. Syst.* **1998**, *15*, 1–56.
3. Uchida, A.; Shinto, Y.; Araki, N.; Ono, K. *J. Orthop. Res.* **1992**, *10*, 440–445.
4. Itokazu, M.; Sugiyama, T.; Ohno, T.; Wada, E.; Katagiri, Y. *J. Biomed. Mater. Res.* **1998**, *39*, 536–538.
5. Benghuzzi, H. A.; Bajpai, P. K.; England, B. G. *Biomed. Sci. Instrum.* **1990**, *26*, 141–149.
6. Benghuzzi, H. A.; Bajpai, P. K.; England, B. G. *Biomed. Sci. Instrum.* **1991**, *27*, 197–203.
7. Otsuka, M.; Sawada, M.; Matsuda, Y.; Nakamura, T.; Kokubo, T. *Biomaterials* **1997**, *18*, 1559–1564.
8. Solberg, B. D.; Gutow, A. P.; Baumgaertner, M. R. *J. Orthop. Trauma* **1999**, *13*, 102–106.
9. Paul, W.; Jerry, N.; Sharma, C. P. *J. Biomed. Mater. Res.* **2002**, *61*, 660–662.
10. Seeherman, H.; Wozney, J. M. *Cytok. Growth Fact. Rev.* **2005**, *16*, 329–345.
11. Ginebra, M. P.; Traykova, T.; Planell, J. A. *J. Controlled Release* **2006**, *113*, 102–110.
12. Jansen, J. A.; Vehof, J. W. M.; Ruhé, P. Q.; Kroeze-Deutman, H.; Kuboki, Y.; Takita, H.; Hedberg, E. L.; Mikos, G. A. *J. Controlled Release* **2005**, *101*, 127–136.
13. Hutmacher, D. W. *Biomaterials* **2000**, *21*, 2529–2543.
14. Alvarez, H.; Castro, C.; Moujir, L.; Perrera, A.; Delgado, A.; Soriano, I.; Evora, C.; Sanchez, E. E. *J. Biomed. Mat. Res. B. Appl. Biomat.* **2008**, *85*, 93–104.
15. Soriano, I.; Evora, C. *J. Controlled Release* **2000**, *68*, 121–134.
16. Soriano, I.; Martin, A. Y.; Evora, C.; Sanchez, E. *J. Biomed. Mater. Res. A* **2006**, *77*, 628–632.
17. Lawson, A. C.; Czernuszka, J. T. *Proc. Inst. Mech. Eng. Part H-J. Engin. Med.* **1998**, *212*, 413–425.
18. Muzzarelli, C.; Muzzarelli, R. A. A. *J. Inorg. Biochem.* **2002**, *92*, 89–94.
19. Shahidi, F.; Abouzaytoun, R. *Adv. Food Nutr. Res.* **1995**, *49*, 93–135.
20. Kumar, M. N.; Muzzarelli, R. A.; Muzzarelli, C.; Sashiwa, H.; Domb, A. J. *Chem. Rev.* **2004**, *104*, 6017–6084.
21. Vongchan, P.; Sajomsang, W.; Subyen, D.; Kongtawelert, P. *Carbohydr. Res.* **2002**, *337*, 1233–1236.
22. Zhang, C.; Ping, Q.; Zhang, H.; Shen, J. *Carbohydr. Polym.* **2003**, *54*, 137–141.
23. Nancollas, G. H.; Mohan, M. S. *Arch. Oral Biol.* **1970**, *15*, 731–745.
24. British Pharmacopoeia **2007**. Appendix XII B. Dissolution: Dissolution test for tablets and capsules (dissolution test for solid dosage forms).
25. Samuels, R. *J. Polym. Sci. Polym. Phys. Ed.* **1981**, *19*, 1081–1105.
26. Kim, C. H.; Choi, K. S. *J. Ind. Eng. Chem.* **2002**, *8*, 71–76.
27. Muzzarelli, R. R. A. A.; Tanfani, F.; Emanuelli, M.; Mariotti, S. *J. Membr. Sci.* **1983**, *16*, 295–308.
28. Siepmann, J.; Peppas, N. A. *Adv. Drug Delivery Rev.* **2001**, *48*, 139–157.
29. Hixson, A. W.; Crowell, J. H. *Ind. Eng. Chem.* **1931**, *23*, 923–931.
30. Varshosaz, J.; Keihanfar, M. *J. Microencapsul.* **2001**, *18*, 277–284.
31. Ritger, P. L.; Peppas, N. A. *J. Controlled Release* **1987**, *5*, 23–36.
32. Higuchi, T. *J. Pharm. Sci.* **1961**, *50*, 874–875.
33. Higuchi, T. *J. Pharm. Sci.* **1963**, *52*, 1145–1149.
34. Wagner, J. G. *J. Pharm. Sci.* **1969**, *58*, 1253–1257.
35. Baker, R. W.; Lonsdale, H. K. Controlled release: mechanisms and rates. In *Controlled Release Of Biologically Active Agents Advances in Experimental Medicine and Biology*; Tanquary, A. C., Lacey, R. E., Eds.; Plenum Press: NY, 1974; Vol. 47, pp 15–72.
36. Yuskel, N.; Kanik, A. E.; Baykara, T. *Int. J. Pharm.* **2000**, *209*, 56–67.
37. Yasvanth, R. G.; Lal Kaul, A. C.; Panchagnula, R. *Pharm. Technol.* **2005**, 68–86.
38. Lavertu, M.; Xia, Z.; Serreqi, A. N.; Berrada, M.; Rodrigues, A.; Wang, D.; Buschmann, M. D.; Gupta, A. *J. Pharm. Biomed. Anal.* **2003**, *32*, 1149–1158.